ORIGINAL RESEARCH ARTICLE

Effect of Hot-Rolling Deformation on Microstructure and Sliding Wear of High-Chromium Cast Iron

Guofeng Yuan, Chengqi Yan, Han He, Shaohua Du, Shun Zhang, and Qi Zhang

Sandwich-structured composite plates, in which high-chromium cast iron (HCCI) was cladded by low-carbon steel (LCS), were newly prepared by a hot-rolling process at different reduction rates. The effects of hot-rolling deformation on the microstructure and sliding wear behavior of HCCI were investigated. Experimental results revealed that the brittle HCCI core layer exhibited good thermoplastic deformation performance when the sandwich structure was hot-rolled at 1150 °C. The thermomechanical treatment not only caused the fracture of Cr-carbides in HCCI, but also made the long axis of Cr-carbide rods parallel to the wear surface. The high area fraction of Cr-carbides and precipitation of secondary carbides improved the wear performance of HCCI. Both the hot-rolled and heat-treated specimens showed better wear resistance than as-cast iron. However, the wear resistance of the hot-rolled specimens decreased as the cumulative reduction rate increased, which is attributed to the synergistic effect of crack propagation and the high area fraction of carbide cavities.

1. Introduction

With excellent wear resistance, high-chromium cast iron (HCCI) is commonly used to prepare equipment parts subject to wear, such as hammers, crusher jaw plates and the roll shaft of a rolling mill (Ref 1-3). HCCI contains a large quantity of primary and eutectic Cr-carbides that have a hardness of 1300-1800 HV. These Cr-carbides endow HCCI with good wear resistance, but at the same time, increase its brittleness and vulnerability to cracking. Recently, many scholars have made attempts to improve the properties of HCCI through the micro-alloying method (Ref 4, 5), heat-treatment (Ref 6), the adjustment of cast processes (Ref 7-9), etc. Plastic deformation is an effective way to enhance the microstructure of a material. However, because of the inherent brittleness of HCCI, few researchers have refined the microstructure of HCCI through thermal deformation processes such as rolling and forging.

Laminated composite materials, which combine the advantages of two metals, have attracted great attention by virtue of their excellent mechanical properties (Ref 10, 11). Recently, due to its good comprehensive mechanical properties, the HCCI and low-carbon steel (LCS)-laminated composite plate has become the focus of research. In the bimetallic composites, HCCI functions as a wear-resistant component and LCS as a ductile component. The common preparation method of HCCI/

LCS composites include duo-casting (Ref 12-17), hot pressing diffusion (Ref 18, 19), powder metallurgy (Ref 20), centrifugal casting combined with hot-rolling (Ref 21, 22), surfacing compound (Ref 23, 24), etc.

Sallam et al. (Ref 14) fabricated an HCCI (19.2 wt.%Cr) and AISI4140 steel composite through the duo-casting method, and the two metals in the composite material prepared achieved a good metallurgical bond. Eroglu et al. (Ref 18) investigated the effects of temperature and holding time on the diffusion bonding between HCCI and LCS. Gao et al. (Ref 19) proposed a hot compression bonding process for the preparation of LCS and HCCI composites. They found that the HCCI core layer flew like a ductile material and deformed simultaneously with the ductile LCS layer. Similarly, Xie et al. (Ref 21) and Liu et al. (Ref 22) prepared a sandwich-structured (LCS/HCCI/LCS) composites through the duo-casting and hot-rolling processes. The results revealed that the soft LCS cladding layer served as a ''lubricant'' during the hot-rolling process, improving the thermomechanical deformation performance of the brittle HCCI layer. Moreover, during hot-rolling deformation, Cr-carbides fractured and dissolved, showing significant changes in morphology. However, the influence of thermomechanical treatment on the wear properties of hot-rolled HCCI has not been thoroughly investigated so far.

In recent years, the preparation of laminated metal composites by the rolling process has drawn considerable attention of researchers. Hot-rolling bonding is a typical method to prepare the laminated bimetal composite (Ref 25, 26). Due to high brittleness and crack sensitivity of HCCI, little is known about the hot-rolling approach to preparing HCCI/LCS bimetallic composites.

On the basis of the previous research, sandwich-structured bimetal composites, in which HCCI was cladded by LCS, were newly prepared by the hot-rolling bonding process at different reduction rates in this study. Moreover, the effect of the cumulative reduction rate on the microstructure of HCCI was analyzed in detail. At the same time, the friction and sliding

Guofeng Yuan, Chengqi Yan, Han He, Shaohua Du, Shun Zhang, and **Qi Zhang**, School of Mechanical Engineering, Anyang Institute of Technology, Anyang 455000, China. Contact e-mail: aygxyygf@163.com.

wear behavior of the hot-rolled HCCI at different cumulative reduction rates was examined using a pin-on-disc type wear tester.

2. Material and Experimental Procedure

The materials studied in the present work were the as-cast HCCI and commercial LCS (Q235). The nominal chemical compositions of the two materials in weight percentage are summarized in Table 1.

The HCCI and LCS plates for hot rolling were cut into specimens of 150 mm × 100 mm × 5 mm in dimension. Before hot rolling, the bonding surfaces of the plates were polished with a steel brush and cleaned with absolute ethyl alcohol. As illustrated in Fig. 1, a sandwich structure was created by cladding both sides of the HCCI plate with LCS plates. Afterward, the treated plates were welded together. The air in the bonding surfaces was pumped out from the reserve tube. The vacuum tube was sealed by hot pressing once the vacuum level dropped below 1.0×10^{-3} Pa. The LCS/HCCI/LCS composite slab was preheated to 1150 °C and held at that temperature for 30 min prior to rolling at a speed of 0.1 m s^{-1} and a cumulative reduction rate of 30, 40 or 50%. After hot rolling, the slabs were air-cooled. In practice, the upper LCS layer can be removed via machining or it may be worn out during use. In the remaining HCCI/LCS laminated composite plate, the HCCI layer plays a wear-resistant role and the LCS layer acts as a ductile component.

A pin-on-disc configuration (Rtec, MFT-5000) was used in the sliding wear tests of the slabs in the absence of lubrication. The wear test samples were cut from the center of the hot-rolled sheet along the rolling direction (RD) and normal direction (ND). For each hot-rolled composite material, the wear test was conducted on the surface of the hot-rolled HCCI layer. Thus, the upper LCS layer was removed by the wire electrical discharge machining process to expose the fresh surface of the hot-rolled HCCI layer. The wear properties of as-cast, heat-treated and hot-rolled samples were compared and analyzed. Before the wear test, each specimen was ground and polished to achieve a roughness level of 1 μm. A Si$_3$N$_4$ ball with a diameter of 6.35 mm was used in the test as the slider ball. The hardness of the Si$_3$N$_4$ ball is $\sim$ 75 HRC. The normal axial load applied was 60 N, the wear track was 4 mm, the constant sliding speed was 8 mm s^{-1}, and the total test time was 30 min. Figure 2 shows the schematic diagram of the pin-on-disc configuration. The wear rate was calculated as follows (Ref 27):

$$W = \frac{bhl}{L} \qquad \text{(Eq 1)}$$

where b, h and l are the width, depth and length of the wear track, respectively. L is the total sliding distance. The values of b and h were the average of five different sites on the wear track measured by a 3D surface profiler (Keyence VXH-2000). In order to obtain more accurate values, each specimen was tested three times in the same wear conditions. The friction coefficient was measured by an analog to digital converter and recorded in a computer.

An optical microscope (OM) and a scanning electron microscope (SEM, ZEISS SIGMA-300) were utilized to examine the microstructure of HCCI. The phase components of HCCI were analyzed by an x-ray diffractometer (XRD). The morphology of the wear surface and subsurface of the specimens were observed via digital microscope (DM, Keyence VXH-2000) and the SEM.

3. Results and Discussion

3.1 Microstructure

Figure 3(a) displays the macrograph of the bimetal material after it was hot-rolled at a cumulative reduction rate of 30%. A sandwich-structured composite with an HCCI core layer was clearly observed. Macroscopically, the two metals were well bonded without macroscopic cracks or holes at the interface. The brittle HCCI core layer was uniformly deformed and free of cracks. As a contrast, the monolithic HCCI plate was hot-rolled at 1150 °C and a cumulative reduction rate of 30%. As shown in Fig. 3(b), many macroscopic cracks were formed in the hot-rolled monolithic HCCI plate. Owing to high crack sensitivity and brittleness, the monolithic HCCI sheet often exhibits poor thermal deformation performance (Ref 28, 29).

The microstructure of as-cast HCCI materials was characterized by the presence of numerous hexagonal primary carbides and finely distributed eutectic carbides (Fig. 4a). HCCI possessed excellent wear resistance on account of the hard Cr-carbides present in it. Nonetheless, the high volume fraction of Cr-carbides amplified the risk of brittle fracture under impact. The main phases in as-received HCCI were retained austenite, martensite and M$_7$C$_3$ carbides (Fig. 4b). The microstructure of the sample heat-treated at 1150 °C was similar to that of as-cast iron. After heat treatment, the sharp corners of Cr-carbides in HCCI were rounded. Some carbides dissolved, and bulk carbides were irregularly distributed in the matrix (Ref 22).

After the hot-rolling treatment, the morphology of Cr-carbides altered evidently (Fig. 5). The eutectic and primary carbides were fractured and broken into pieces. Partially broken primary carbides were completely encapsulated by the ferrite matrix and flew with it. The fractured Cr-carbides in HCCI during hot rolling promoted the coordinated deformation of Cr-carbides and the matrix. However, some micro-voids were formed in partially fractured carbides, as indicated by red circles in Fig. 5. During the thermoplastic deformation process,

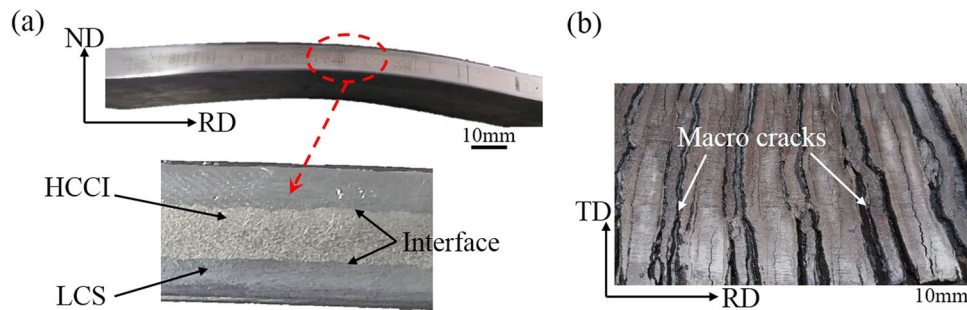**Table 1 Chemical compositions (wt.%) of HCCI and LCS**

Material	C	Si	Cr	Mn	P	S	Mo	Ni	Fe
HCCI	2.8	1.1	28	1.0	0.02	0.02	0.5	0.4	Balance
LCS	0.12	0.2	0.1	0.5	0.01	0.002	…	…	Balance
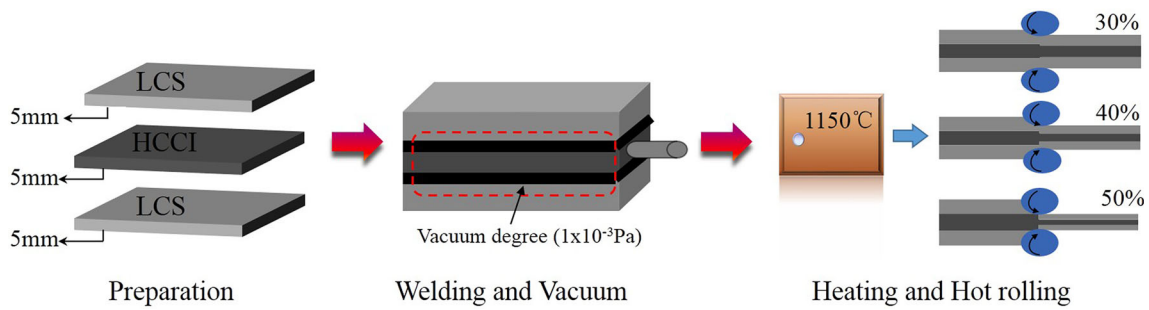
Fig. 1 Schematic diagram of the bimetallic assembly and the experimental process
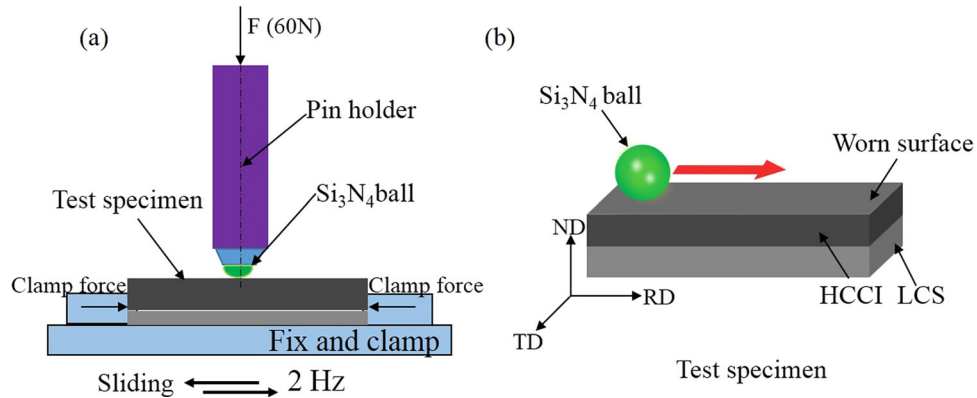
Fig. 2 Schematic diagram of the pin-on-disc apparatus

Fig. 3 Macrograph of the hot-rolled plate at 1150 °C/30% accumulated reduction rate: (a) the hot-rolled sandwich-structured composite and (b) the monolithic HCCI plate

micro-cracks first occurred in the hard and brittle Cr-carbides and then expanded with the increase in the cumulative reduction rate, forming large crack gaps. Some crack gaps were filled by the nearby austenite matrix or fine eutectic carbides, but some could not be filled in time during the flow deformation process. As a result, micro-voids were formed in fractured Cr-carbides.

An EBSD analysis was made to further investigate the microstructure of hot-rolled HCCI. Figure 6 shows the band contrast maps and phase maps of hot-rolled HCCI. In the phase maps, yellow, red and blue colors represent M_7C_3 carbide, martensite and austenite, respectively. It can be seen from the phase maps that M_7C_3 carbides were distributed in the matrix as an irregular hexagon or short rod. After the hot-rolling process, micro-cracks occurred in some primary carbides, which were then fractured into small blocks and dispersed in the matrix. The fragmentation degree of the carbides increased

significantly as the cumulative reduction rate was raised to 50%. In addition, the fractured primary and eutectic carbides had a tendency to flow and align along the rolling direction. To refine the carbides by fracturing them can reduce the shearing effect on the matrix and improve the overall toughness of HCCI (Ref 12)

According to Fig. 4b, the as-cast HCCI mainly contained M_7C_3 carbides, retained austenite, and martensite. Figure 7 describes the effect of hot rolling on the HCCI microstructure. The phase components of the hot-rolled HCCI were similar to those of the as-cast one, except that the peak intensity of $M_{23}C_6$ type secondary carbides in the hot-rolled HCCI increased. Moreover, the austenite peaks were also slightly intensified in HCCI hot-rolled at 1150 °C. Tabrett et al. (Ref 30) reported that as the destabilization temperature rose, the solubility of C atoms in austenite increased, the temperature for austenite to transform into martensite declined, and the driving force of
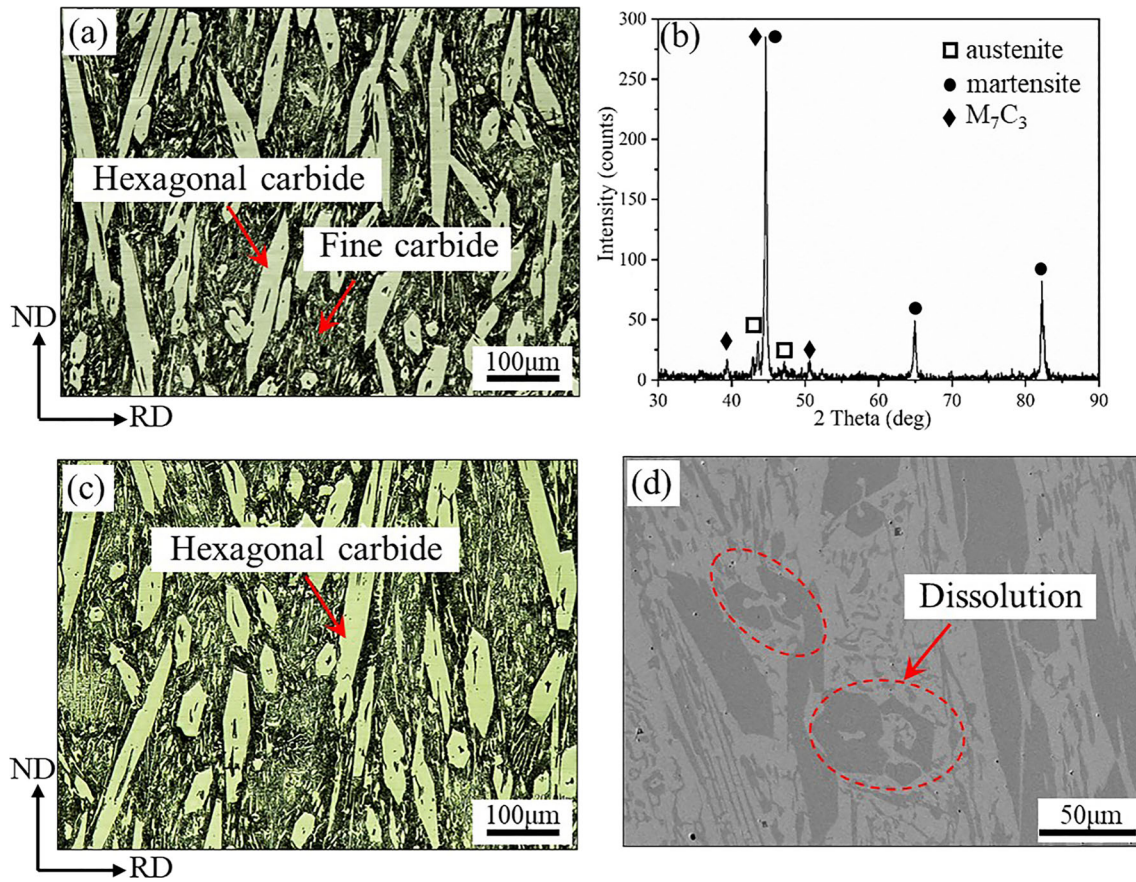
Fig. 4 The initial microstructure of the as-cast HCCI: (a) OM micrograph and (b) the x-ray diffraction pattern; microstructure of the sample after heat treatment at 1150 °C: the microstructure of the heat-treated HCCI: (c) OM micrograph and (d) SEM micrograph
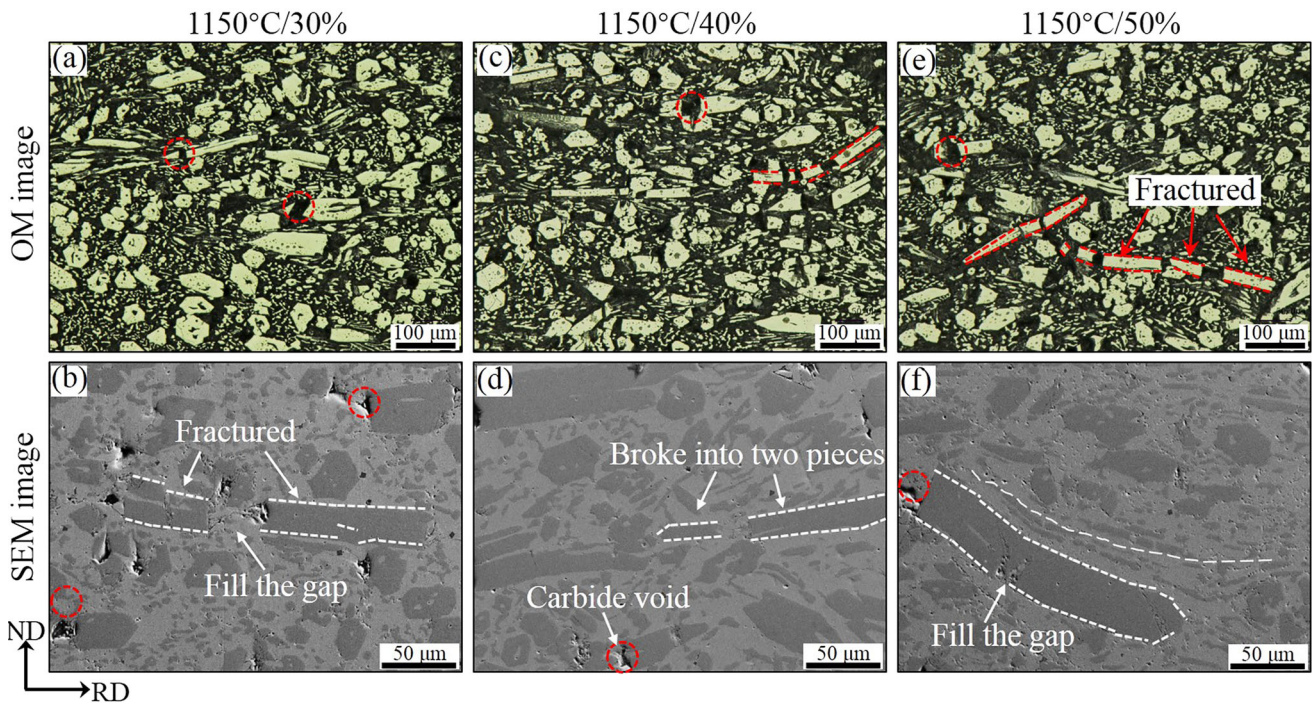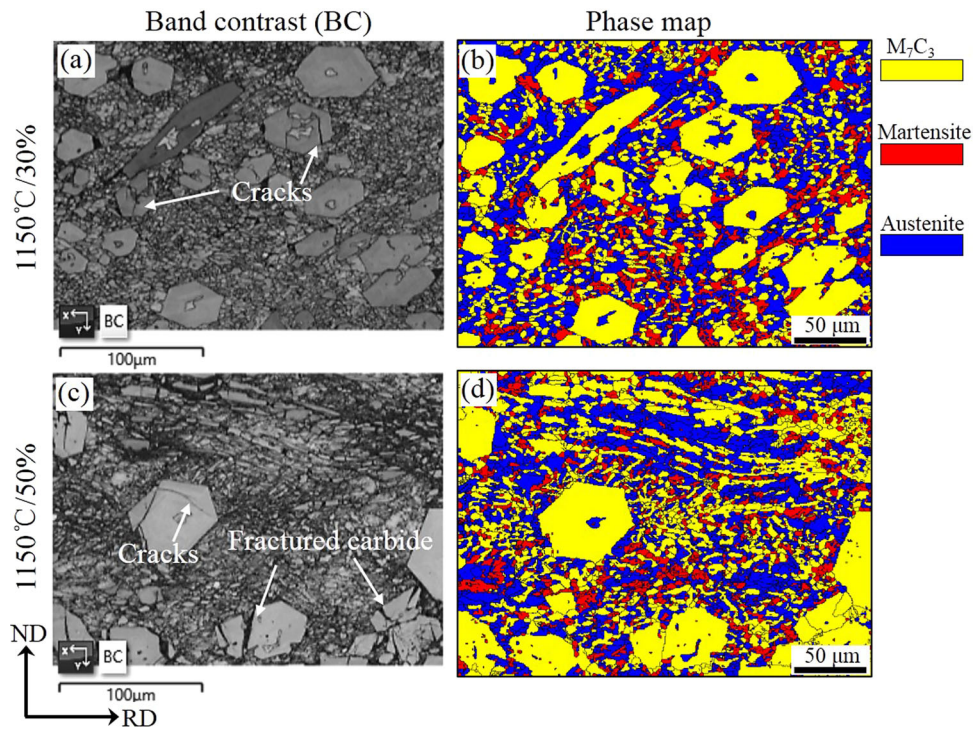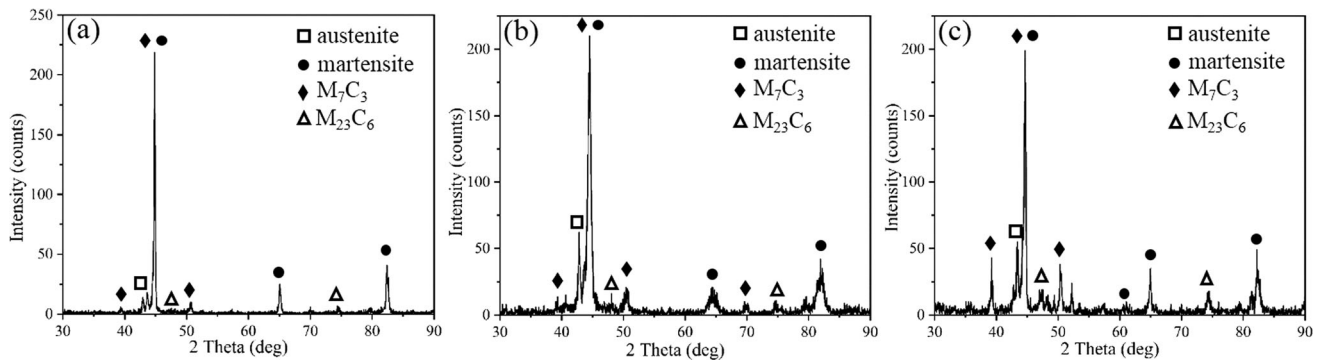

Fig. 5 OM and SEM micrographs of the hot-rolled HCCI with different reduction rates: (a) and (b) 30%, (c) and (d) 40%, (e) and (f) 50%

Band contrast (BC)　　　　Phase map

(a) 1150°C/30% — Cracks　　(b) M7C3 / Martensite / Austenite — 50 μm — 100μm

(c) 1150°C/50% — Cracks, Fractured carbide　　(d) — 50 μm — 100μm

ND / RD

Fig. 6 EBSD analysis results: (a) and (c) the band contrast maps, (b) and (d) the phase maps

Fig. 7 XRD patterns of the hot-rolled HCCI with different reduction rates: (a) 30%, (b) 40% and (c) 50%

carbide precipitation decreased. As a result, the retained austenite content increased.

3.2 Sliding Wear Behavior

Since the specimens were rubbed with a Si_3N_4 ball, the wear tracks on the surface presented a bow-shaped cross section (Fig. 8a). The width and depth of the tracks varied among the five specimens in the same wear conditions, which indicated these specimens had different wear resistance. Figure 8a shows the depth profiles of the wear tracks. The hot-rolled specimen at the cumulative reduction rate of 30% had the smallest wear depth, while the as-cast specimen had the largest wear depth.

The average wear rates of the five specimens are summarized in Fig. 8b. Both thermomechanical and heat treatments improved the wear resistance of HCCI. The wear rate of the as-cast specimen was higher than that of both hot-rolled and heat-treated HCCI. However, with the increase in the cumulative reduction rate, the wear resistance of the hot-rolled specimen decreased. This phenomenon is mainly ascribed to the

microstructure evolution of HCCI at different cumulative reduction rates.

Figure 9 shows the coefficient of friction (COF) as a function of the wear time for test specimens. The COFs of the five specimens have a similar trend. The wear process can be divided into two stages according to the change process of the COF curves. The first stage is the running-in stage, during which the COF fluctuated sharply. The second stage corresponds to the steady state of the specimen, during which the COF was stable (Ref 31, 32). At the beginning of the tests, the contact area between the specimen and the pin was small. Hence, the COF was small and unstable in this stage. The COF increased with the enlarged wear area (Ref 33). During the running-in process, the wear surface would undergo microstructure evolution, thermal change and chemical reactions, and especially oxides would produce. When the test was run for approximately 800 s, the wear process reached a steady state. For the specimens prepared at 30 and 40% reduction rates, their COF maintained at ~ 0.5, whereas the COF of as-

(a)

(b)
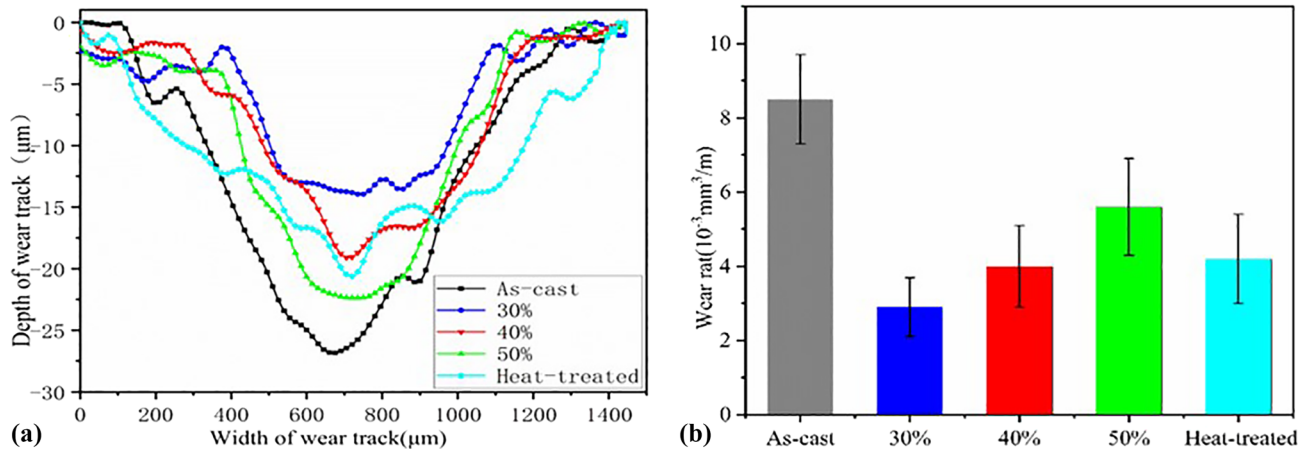
Fig. 8 (a) Depth profile of the wear tracks and (b) wear rate of the as-cast HCCI, heat-treated and the hot-rolled specimens
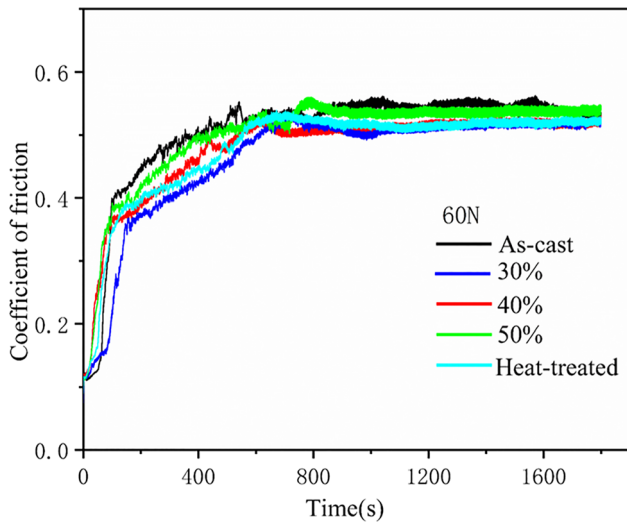
Fig. 9 Coefficient of friction as a function of the wear time

cast iron and the specimen prepared at the reduction rate of 50% was slightly higher.

3.3 Wear Property Analysis of HCCI

In the thermomechanical treatment process, the microstructure of HCCI underwent great changes, especially the size and distribution morphology of carbides. Specifically, the carbides in HCCI were fractured and defects such as micro-voids or micro-cracks were formed (Fig. 5 and 6).

Figure 10(a) and (b) shows the OM images of the wear surface (RD-TD section) of the as-cast specimen and the specimen hot-rolled at the reduction rate of 50%. The distribution morphologies of carbides on the wear surface differed greatly before and after the hot-rolling treatment. After hot rolling, the long axis of some carbides became parallel to the RD-TD section, leading to a change in the area fraction of hard carbides on the wear surface. The area fraction of Cr-carbides in the test specimens was measured using the software "Image Pro". The results were obtained by 10 measurements on micrographs magnified 200 times. The area fraction of Cr-carbides on the wear surface of the hot-rolled specimens was higher than that of the as-cast and heat-treated specimens

(Fig. 10d). A high area fraction of hard Cr-carbides provided protection for the HCCI against wear and improved its wear performance (Ref 34).

Meanwhile, the microstructure of the matrix and the precipitation of secondary carbides also had remarkable effects on the wear properties of HCCI. Figure 11 shows the TEM micrograph of the secondary carbides of the HCCI hot-rolled at the reduction of 50%. The secondary carbides were distributed at the grain boundary of the matrix in the form of spherical particles, with a size of about 200-600 nm. XRD pattern and diffraction spot analysis revealed that the secondary carbide was $M_{23}C_6$. The Cr-carbides in HCCI would fracture and dissolve during thermoplastic deformation, promoting the generation of a saturated solid solution of Cr elements in the matrix. During the cooling process, supersaturated Cr atoms and C atoms in the matrix precipitated to form secondary carbides with the decrease in solubility (Ref 31). These secondary carbides have higher hardness and play a dispersive strengthening effect on the matrix, which effectively improves the strength and wear properties of HCCI.

Figure 10c shows the SEM image of carbide cavities in the specimen hot-rolled at the reduction rate of 50%. There were cavities and micro-cracks in the fractured carbides. More carbide cavities were formed with the increase in the cumulative reduction rate (Fig. 10d). A distinctive feature of HCCI was the high content of hard carbides embedded in the ferrite matrix, so there were a lot of bonding interfaces between the carbide and the matrix. At the same time, the fractured carbide was wrapped by the matrix, forming new bonding interfaces. When the gap in the fractured carbide was not fully filled, defects such as carbide cavities or micro-cracks were generated, which destroyed the microstructural of HCCI, and reduced the effective bonding area between the hard carbide and matrix. This would result in reduced wear properties of HCCI.

3.4 Sliding Wear Mechanism Analysis of HCCI

The wear surface morphologies of the test specimens are displayed in Fig. 12. On the wear surface of the test specimens, there were small grooves formed by micro-cutting and pits formed by hard carbide spalling. During the sliding wear test, there were alternating compressive and tensile stresses generated on the specimen surface and the ball, resulting in low-frequency fatigue. Brittle Cr-carbides were spalled once the
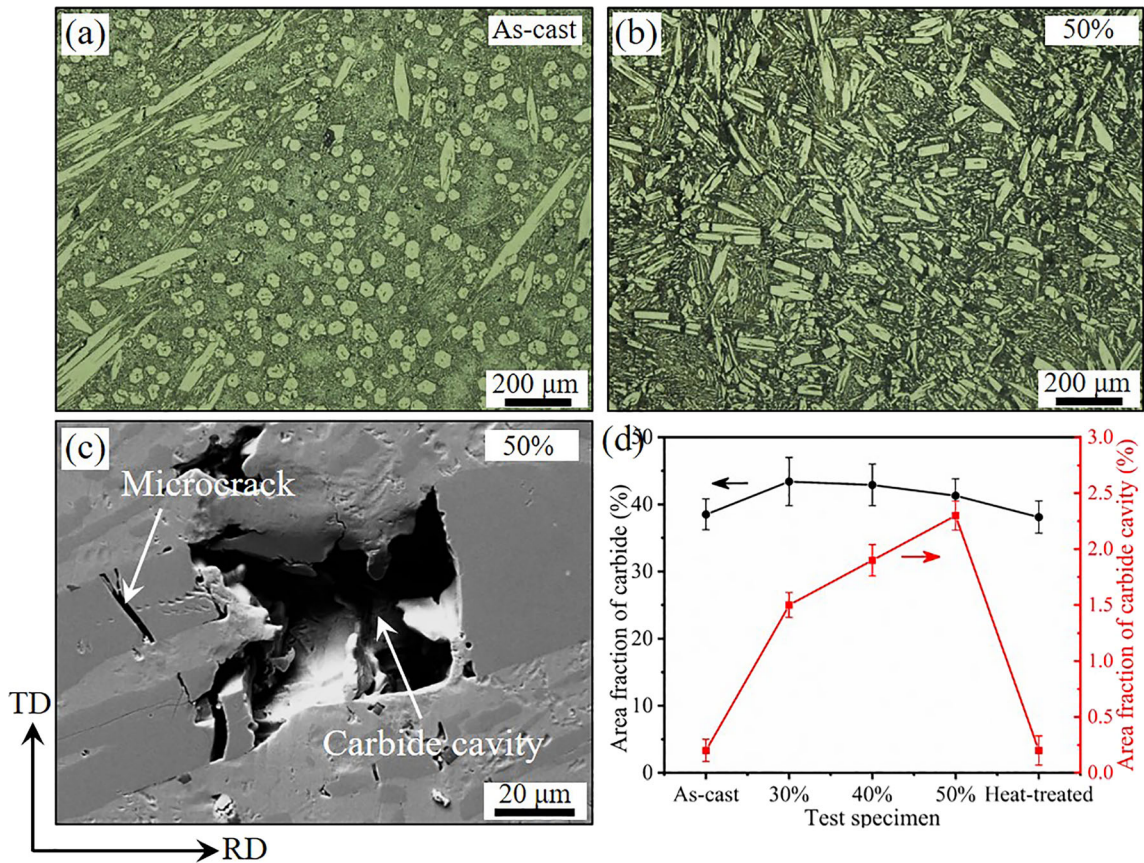
Fig. 10 OM image of the wear surface: (a) as-cast, (b) 50%; (c) SEM image of carbide cavity of 50% specimen; (d) the area fraction of carbide and carbide cavity of HCCI in different treatment states
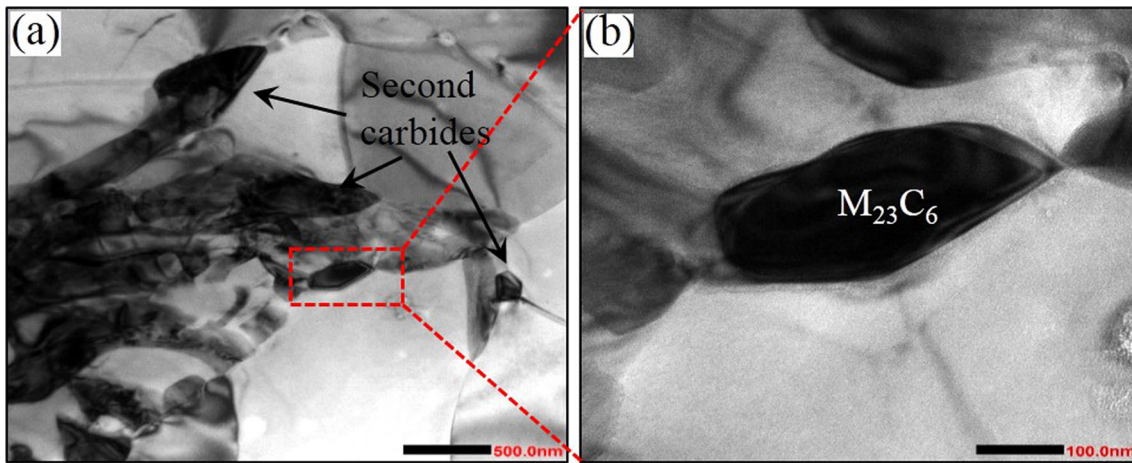

Fig. 11 Second carbides of the 50% hot-rolled HCCI: (a) TEM micrograph of the second carbides and (b) the enlarged photograph of the red box in figure a

contact stress exceeded their strength of Cr-carbides. The falling carbide blocks acted as abrasives, producing a three-body abrasive wear force that accelerated the wear of the specimen. According to Fig. 12, the as-cast specimen was more severely worn, with many flakes of carbides exfoliating from the wear surface. The hot-rolled specimens had better wear resistance than the as-cast specimens. However, the hot-rolled specimen surface was worn more severely increased with the increase in the cumulative reduction rate. The reason is that the

carbide cavities and micro-cracks formed after hot rolling made it easy for the carbides to flake off the matrix.

To better analyze the sliding wear mechanism of HCCI, the subsurface of the wear track was observed under an SEM, and the results are shown in Fig. 13. It is evident that the carbides on the subsurface of the wear track were broken to varying degrees, and the micro-cracks expanded in the carbides. The carbide exfoliation on the wear surface was more serious in the as-cast specimens (Fig. 13a). The wear surface of the specimen
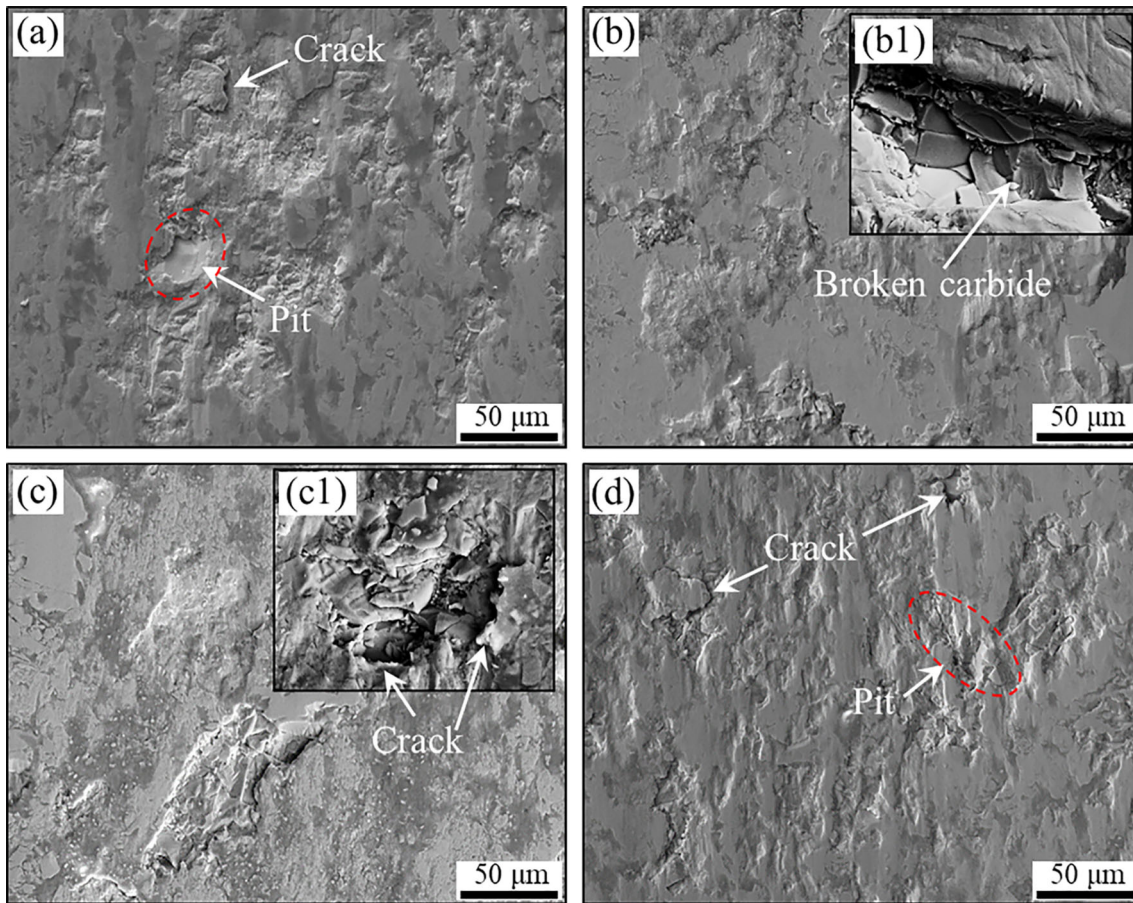
Fig. 12 Wear morphologies of the test specimens: (a) as-cast HCCI, (b) and (b1) 30%, (c) and (c1) 40%, (d) 50%
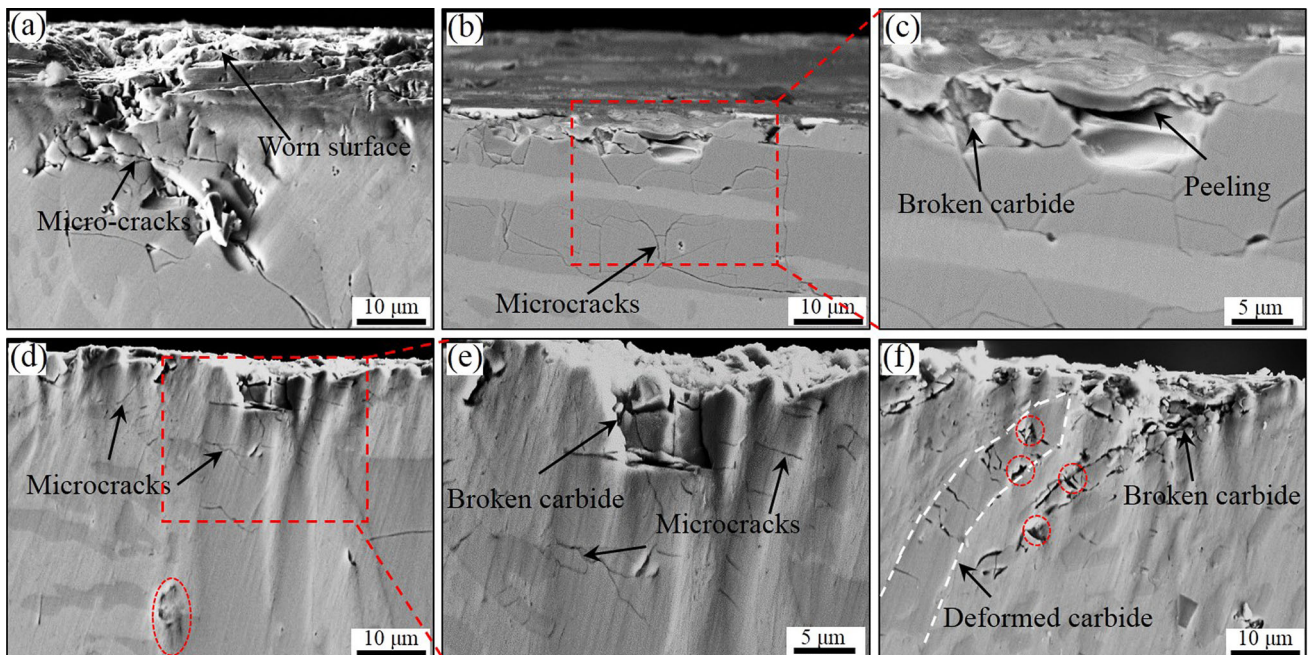
Fig. 13 SEM images of the subsurface of the sliding scar of the test specimens: (a) as-cast iron, (b) 30%, (c) the enlarged photograph of the red box in figure b, (d) 40%, (e) the enlarged photograph of the red box in figure d and (f) 50%

hot-rolled at the reduction rate of 30% was relatively flatter and covered with a thin oxide film, which was formed by thermal deformation and chemical oxidation (Ref 33). Gao et al. (Ref 34) proved that the thin oxide film was formed on the HCCI surface during dry friction sliding, and it served as a lubricant in the wear process. In the profile micrographs of the specimens hot-rolled at the reduction rate of 40 and 50%, some pits were observed in the fractured carbides on the wear surface. The gap between carbides in the pits was large, and the carbides tended to separate from each other and peel off the wear surface. Under the periodic tensile stress and compressive stress applied by the Si_3N_4 ball, these micro-gaps and pits were more likely to expand, resulting in a decrease in the binding strength between the matrix and the carbide.

Based on the above analysis, the wear mechanisms of as-cast iron and the hot-rolled specimens were obtained (Fig. 14). The microstructure of HCCI can be regarded as a particle-reinforced composite composed of hard Cr-carbides and the soft ferrite matrix. The hard carbide protected the iron matrix, which supported the carbide in turn, greatly improving the wear resistance of HCCI. During the sliding wear process, the ferrite matrix was first worn away, and the hard carbide protruded from the surface to protect the matrix. Under the action of periodic tensile stress and compressive stress applied by the Si_3N_4 ball, the protruding carbide was broken and fell, forming some micro-cracks on the subsurface (Fig. 14a).

The high area fraction of carbides on the wear surface and the crack-resistant ability of the matrix were the main contributors to the good wear properties of HCCI. After hot rolling, the carbide particles were refined and the area fraction of carbides on the wear surface increased. Consequently, they could effectively protect the iron matrix from abrasion. At the same time, the precipitation of secondary carbides and the increase in residual austenite content also played a role in improving the wear resistance of the matrix. Therefore, the wear properties of hot-rolled specimens were better than those of the as-cast specimen.

However, carbide cavities or micro-gaps were also formed after hot rolling, especially at higher reduction rates (Fig. 14b, c). The formation of these defects weakened the support to the hard carbide by the matrix. When the ball slid on the specimen surface, the carbide peeled off from the wear surface earlier under the synergistic effect of crack propagation in the carbide and the increasing number of carbide cavities. Moreover, the falling fine carbide particles acted as three-body abrasives, which accelerated the wear rate (Fig. 14c). Therefore, the wear
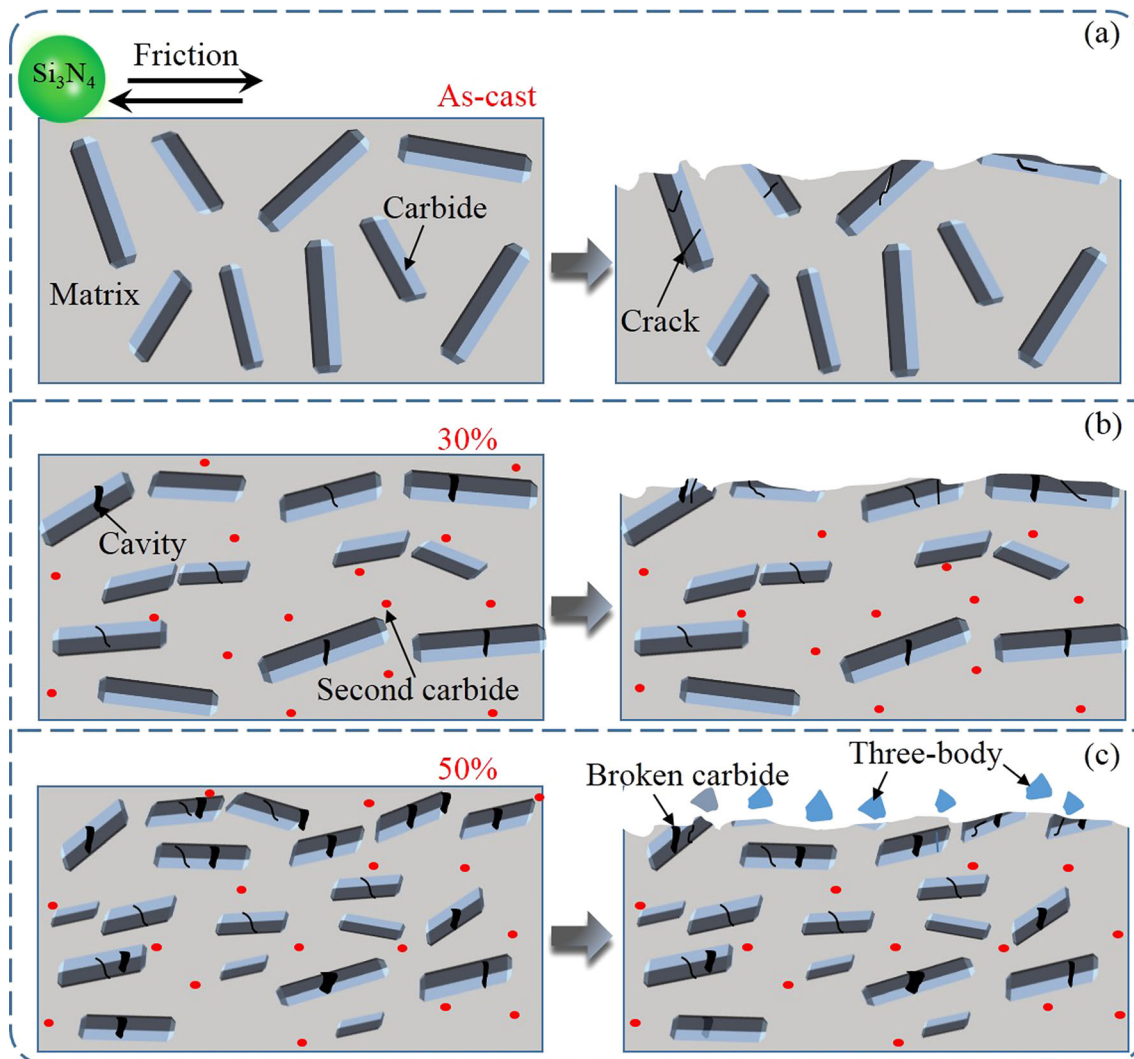
Fig. 14 Schematic description of the wear mechanism of the as-cast HCCI and hot-rolled HCCI: (a) as-cast iron, (b) 30% and (c) 50%

resistance of the hot-rolled specimen decreased with the increase in the cumulative reduction rate.

4. Conclusions

A sandwich-structured composite material, in which HCCI was cladded by LCS, was newly prepared by the hot-rolling bonding process at different reduction rates. The microstructure and sliding wear behavior of HCCI were investigated. The following conclusions are drawn.

1. The brittle HCCI core layer showed good thermomechanical deformation performance when the sandwich structure was hot-rolled at 1150 °C. The fractured carbides were wrapped by the matrix and flew along the rolling direction with the matrix. However, some defects such as carbide cavities and micro-cracks were formed in the fractured carbides.
2. The wear resistance of hot-rolled HCCI was better than that of as-cast HCCI. With the increase in the cumulative reduction rate, the wear resistance of the hot-rolled specimen decreased.
3. The long axis of carbide rods became parallel to the wear surface after the hot rolling treatment, leading to an increased fraction of carbides on the wear surface. A high area fraction of carbides provided protection for the matrix against wear and improved its wear performance.
4. The wear morphology of the sample were dominated by carbides spalling, and the carbides on the subsurface of the wear track were broken to varying degrees. The defects such as carbide cavities and micro-cracks impaired the wear resistance of HCCI.

References

1. X.H. Tang, R. Chung, D.Y. Li, B. Hinckley and K. Dolman, Variations in Microstructure of High Chromium Cast Irons and Resultant Changes in Resistance to Wear, Corrosion and Corrosive Wear, *Wear*, 2009, **267**, p 116–121. https://doi.org/10.1016/j.wear.2008.11.025
2. S.D. Carpenter, D. Carpenter and J.T.H. Pearce, XRD and Electron Microscope Study of an As-Cast 26.6% Chromium White Iron Microstructure, *Mater. Chem. Phys.*, 2004, **85**, p 32–40. https://doi.org/10.1016/j.matchemphys.2003.11.037
3. X.J. Wu, J.D. Xing, H.G. Fu and X.H. Zhi, Effect of Titanium on the Morphology of Primary M_7C_3 Carbides in Hypereutectic High Chromium White Iron, *Mater. Sci. Eng. A*, 2007, **457**, p 180–185. https://doi.org/10.1016/j.msea.2006.12.006
4. X.H. Zhi, J.Z. Liu, J.D. Xing and S.Q. Ma, Effect of Cerium Modification on Microstructure and Properties of Hypereutectic High Chromium Cast Iron, *Mater. Sci. Eng. A*, 2014, **603**, p 98–103. https://doi.org/10.1016/j.msea.2014.02.080
5. H.S. Ding, S.Q. Liu, H.L. Zhang and J.J. Guo, Improving Impact Toughness of a High Chromium Cast Iron Regarding Joint Additive of Nitrogen and Titanium, *Mater. Des.*, 2016, **90**, p 958–968. https://doi.org/10.1016/j.matdes.2015.11.055
6. V. Efremenko, K. Shimizu and Y. Chabak, Effect of Destabilizing Heat Treatment on Solid-State Phase Transformation in High-Chromium Cast Irons, *Metall. Mater. Trans. A*, 2013, **44**, p 5435–5446. https://doi.org/10.1007/s11661-013-1890-9
7. R.J. Chung, X. Tang, D.Y. Li, B. Hinckley and K. Dolman, Effects of Titanium Addition on Microstructure and Wear Resistance of Hypereutectic High Chromium Cast Iron Fe–25wt.%Cr–4wt.%C, *Wear*, 2009, **267**, p 356–361. https://doi.org/10.1016/j.wear.2008.12.061
8. S.Q. Ma, J.D. Xing, Y.L. He, Y.F. Li, Z.F. Huang, G.Z. Liu and Q.J. Geng, Microstructure and Crystallography of M_7C_3 Carbide in Chromium Cast Iron, *Mater. Chem. Phys.*, 2015, **161**, p 65–73. https://doi.org/10.1016/j.matchemphys.2015.05.008
9. S.R. Wang, L.H. Song, Y. Qiao and M. Wang, Effect of Carbide Orientation on Impact-Abrasive Wear Resistance of High-Cr Iron Used in Shot Blast Machine, *Tribol. Lett.*, 2013, **50**, p 439–448. https://doi.org/10.1007/s11249-013-0140-z
10. C. Elanchezhian, B.V. Ramnath, G. Ramakrishnan, K.N. Sripada, M. Mural-idharan and V. Kishore, Review on Metal Matrix Composites for Marine Applications, *Mater. Today. Proc.*, 2018, **5**, p 1211–1218. https://doi.org/10.1016/j.matpr.2017.11.203
11. P.M. Anderson, J.F. Bingert, A. Misra and J.P. Hirth, Rolling Textures in Nanoscale Cu/Nb Multilayers, *Acta Mater.*, 2003, **51**, p 6059–6075. https://doi.org/10.1016/S1359-6454(03)00428-2
12. H. Oh, S. Lee, J. Jung and S. Ahn, Correlation of Microstructure with the Wear Resistance and Fracture Toughness of Duocast Materials Composed of High-Chromium White Cast Iron and Low-Chromium Steel, *Metall. Mater. Trans. A*, 2001, **32**, p 515–524. https://doi.org/10.1007/s11661-001-0068-z
13. C.K. Kim, S. Lee and J.Y. Jung, Effects of Heat Treatment on Wear Resistance and Fracture Toughness of Duo-Cast Materials Composed of High-Chromium White Cast Iron and Low-Chromium Steel, *Metall. Mater. Trans. A*, 2006, **37**, p 633–643. https://doi.org/10.1007/s11661-006-0035-9
14. H.E.M. Sallam, K. Abd EI-Aziz, H. Abd EI-Raouf and E.M. Elabanna, Failure Analysis and Flexural Behavior of High Chromium White Cast Iron and AISI4140 Steel Bimetal Beams, *Mater. Des.*, 2013, **52**, p 974–980. https://doi.org/10.1016/j.matdes.2013.06.045
15. X.F. Xiao, S.P. Ye, W.X. Yin and Q. Xue, HCWCI/Carbon Steel Bimetal Liner by Liquid-Liquid Compound Lost Foam Casting, *J. Iron. Steel Res. Int.*, 2012, **19**, p 13–19. https://doi.org/10.1016/S1006-706X(12)60145-9
16. B.W. Xiong, C.C. Cai, H. Wan and B.P. Lu, Fabrication of High Chromium Cast Iron and Medium Carbon Steel Bimetal by Liquid–Solid Casting in Electromagnetic Induction Field, *Mater. Des.*, 2011, **32**, p 2978–2982. https://doi.org/10.1016/j.matdes.2011.01.006
17. B.W. Xiong, C.C. Cai and B.P. Lu, Effect of Volume Ratio of Liquid to Solid on the Interfacial Microstructure and Mechanical Properties of High Chromium Cast Iron and Medium Carbon Steel Bimetal, *J. Alloy. Compd.*, 2011, **509**, p 6700–6704. https://doi.org/10.1016/j.matdes.2011.01.006
18. M. Eroglu and B. Kurt, Diffusion Bonding Between High Chromium White Iron and Low Carbon Steel, *Mater. Sci. Tech-Lond.*, 2007, **23**, p 171–176. https://doi.org/10.1179/174328407X154202
19. X.J. Gao, Z.Y. Jiang, D.B. Wei, S.H. Jiao, D.F. Chen, J.Z. Xu, X.M. Zhang and D.Y. Gong, Effects of Temperature and Strain Rate on Microstructure and Mechanical Properties of High Chromium Cast Iron/Low Carbon Steel Bimetal Prepared by Hot Diffusion-Compression Bonding, *Mater. Des.*, 2014, **63**, p 650–657. https://doi.org/10.1016/j.matdes.2014.06.067
20. Y.C. Li, M.Y. Gong, K. Wang, P. Li, X. Yang and W.P. Tong, Diffusion Behavior and Mechanical Properties of High Chromium Cast Iron/Low Carbon Steel Bimetal, *Mater. Sci. Eng. A*, 2018, **718**, p 260–266. https://doi.org/10.1016/j.msea.2018.01.111
21. G.L. Xie, J.T. Han, L. Liu and Z.Y. Jiang, Texture, Microstructure and Microhardness Evolution of a Hot-Rolled High Chromium Cast Iron, *Mater. Sci. Eng. A*, 2010, **527**, p 6251–6254. https://doi.org/10.1016/j.msea.2010.06.036
22. F. Liu, Y.H. Jiang, H. Xiao and J. Tan, Study on Fragmentation and Dissolution Behavior of Carbide in a Hot-Rolled Hypereutectic High Chromium Cast Iron, *J. Alloy. Compd.*, 2015, **618**, p 380–385. https://doi.org/10.1016/j.jallcom.2014.07.131

23. A. Jilleh, N.K. Babu, V. Thota, A.L. Anis, M.K. Harun and M.K. Talari, Microstructural and Wear Investigation of High Chromium White Cast Iron Hardfacing Alloys Deposited on Carbon Steel, *J. Alloy. Compd.*, 2021, **857**, 157472. https://doi.org/10.1016/j.jallcom.2020.157472

24. R.N. Jia, S.L. Liu, Z.C. Luo, J.P. Ning, H.Y. Wang, T.G. Luo, Y.S. Zhu, X.S. Yuan and Z. Wang, Microstructure and Wear Resistance of WC and High Chromium Cast Iron Hardfacing Layer, *Coatings*, 2020, **10**, p 852–861. https://doi.org/10.3390/coatings10090852

25. T. Yu, Y.A. Jing, X.L. Yan, W.B. Li, Q.H. Pang and G. Jing, Microstructures and Properties of Roll-Bonded Stainless/Medium Carbon Steel Clad Plates, *J. Mater. Process. Tech.*, 2019, **266**, p 264–273. https://doi.org/10.1016/j.jmatprotec.2018.06.007

26. J. Li, C.R. Liu, Y.H. Song, G.H. Zhao, L.F. Ma and Q.X. Huang, Influence of Hot Rolling + Heat Treatment on Microstructure and Mechanical Properties of NM500/Q345/NM500 Composite Plate, *J. Mater. Sci.*, 2021, **56**, p 6016–6030. https://doi.org/10.1007/s10853-020-05666-4

27. H.Y. Xia, G.J. Qiao, S.L. Zhou and J.P. Wang, Reciprocating Friction and Wear Behavior of Reaction-Formed SiC Ceramic Against Bearing Steel Ball, *Wear*, 2013, **303**, p 276–285. https://doi.org/10.1016/j.wear.2013.03.038

28. Z.Y. Jiang, X.J. Gao, S.L. Li, H.M. Zhang, D.F. Chen and J.Z. Xu, Interface Analysis and Hot Deformation Behaviour of a Novel Laminated Composite with High-Cr Cast Iron and Low Carbon Steel Prepared by Hot Compression Bonding, *J. Iron. Steel Res. Int.*, 2015, **22**, p 438–445. https://doi.org/10.1016/S1006-706X(15)30024-8

29. J.Z. Xu, X.J. Gao, Z.Y. Jiang and D.B. Wei, A Comparison of Hot Deformation Behavior of High-Cr White Cast Iron and High-Cr White Cast Iron/Low Carbon Steel Laminate, *Steel Res. Int.*, 2016, **87**, p 780–788. https://doi.org/10.1002/srin.201500234

30. C.P. Tabrett, I.R. Sare and M.R. Ghomashchi, Microstructure-Property Relationships in High Chromium White Iron Alloys, *Int. Mater. Rev.*, 1996, **41**, p 59–82. https://doi.org/10.1179/imr.1996.41.2.59

31. M. Ruiz-Andres, A. Conde, J.D. Damborenea and I. Garcia, Friction and Wear Behaviour of Dual Phase Steels in Discontinuous Sliding Contact Conditions as a Function of Sliding Speed and Contact Frequency, *Tribol. Int.*, 2015, **90**, p 32–42. https://doi.org/10.1016/j.triboint.2015.03.038

32. H.M. Cao, X. Zhou, X.Y. Li and K. Lu, Friction Mechanism in the Running-in Stage of Copper: From Plastic Deformation to Delamination and Oxidation, *Tribol. Int.*, 2017, **115**, p 3–7. https://doi.org/10.1016/j.triboint.2017.05.027

33. J. Yang, Y. Jiang, J. Gu, Z. Guo and H. Chen, Effect of Austenitization Temperature on the Dry Sliding Wear Properties of a Medium Carbon Quenching and Partitioning Steel, *Acta Metall. Sin.*, 2018, **54**, p 21–30. https://doi.org/10.11900/.0412.1961.2017.00129

34. X.J. Gao, Z.Y. Jiang, D.B. Wei and B. Kosasih, Effect of Thermomechanical Treatment on Sliding Wear of High-Cr Cast Iron with Large Plastic Deformation, *Tribol. Int.*, 2015, **92**, p 117–125. https://doi.org/10.1016/j.triboint.2015.06.002